Cerebral Cortex Advance Access published October 22, 2015

OXFORD

Cerebral Cortex, 2015, 1–11

doi: 10.1093/cercor/bhv243
Original Article

ORIGINAL ARTICLE

Dopaminergic Modulation of the Functional Ventrodorsal Architecture of the Human Striatum

Payam Piray[1], Hanneke E.M. den Ouden[1], Marieke E. van der Schaaf[1,2], Ivan Toni[1] and Roshan Cools[1,2]

[1]Donders Institute for Brain Cognition and Behaviour, Centre for Cognitive Neuroimaging, Radboud University, Nijmegen, The Netherlands and [2]Department of Psychiatry, Radboud University Medical Center, Nijmegen, The Netherlands

Address correspondence to Payam Piray. Email: p.piray@donders.ru.nl

Abstract

Interactions between motivational, cognitive, and motor regions of the striatum are crucial for implementing behavioral control. Work with experimental animals indicates that such interactions are sensitive to modulation by dopamine. Using systematic pharmacological manipulation of dopamine D2-receptors and resting-state functional imaging, we defined the functional architecture of the human striatum and quantified the effects of dopaminergic drugs on intrinsic effective connectivity between striatal subregions. We found that dopamine modulates interactions between motivational and cognitive regions, as well cognitive and motor regions of the striatum. Stimulation and blockade of the dopamine D2-receptor had opposite (increasing and decreasing) effects on the efficacy of those interactions. Furthermore, trait impulsivity was specifically associated with dopaminergic modulation of ventral-to-dorsal striatal connectivity. Individuals with high trait impulsivity exhibited greater drug-induced increases (after stimulation) and decreases (after blockade) of ventral-to-dorsal striatal connectivity than those with low trait impulsivity. These observations establish a key link between dopamine, intrinsic effective connectivity between striatal subregions, and trait impulsivity.

Key words: connectivity, dopamine, functional magnetic resonance imaging, impulsivity

Introduction

The striatum subserves many functions, ranging from incentive motivation to goal-directed action selection and habitual response control, and is implicated in a wide range of neuropsychiatric disorders such as addiction, attention deficit hyperactivity disorder, and Parkinson's disease. These various striatal functions have long been thought to depend on information processing within relatively segregated motivational, cognitive, and motor regions of the striatum (Alexander et al. 1986). However, recent evidence has highlighted an important functional role for interactions between these different regions of the striatum (Haber and Knutson 2010; Aarts et al. 2011). For example, according to current theories of addiction, the transition from impulsive to compulsive drug use corresponds to a transition from ventral to dorsal striatal control of drug-seeking behavior (Everitt et al. 2008). Despite the importance of these hierarchical intrastriatal interactions, they have received little attention in human research.

Neuroanatomical data from nonhuman primates have suggested that the communication between striatal regions is subserved by a network of spiraling connections between the dopaminergic midbrain and the striatum (Haber et al. 2000). Thus, dopamine is ideally suited for mediating information flow along the mediolateral striatal gradient through serial reciprocal connections between the striatum and the midbrain. This hypothesis concurs with evidence from work with behaving rodents, indicating that the transition from impulsive to compulsive drug use, and the corresponding transition of behavioral control from the ventral to the dorsolateral striatum, can be promoted by dopamine (Dalley et al. 2007; Belin and Everitt 2008; Belin et al. 2008).

Here, we aim to assess how dopamine modulates intrinsic human striatal connectivity by administering dopaminergic drugs and by exploiting interindividual variability in the direction and extent of dopaminergic drug effects (Cools and D'Esposito 2011). Individual differences in the personality trait of impulsivity have been shown to correspond with individual differences in dopamine receptor availability (Dalley et al. 2007; Buckholtz et al. 2010) and with the effects of dopaminergic drugs on striatal function (Cools et al. 2007). Specifically, trait impulsivity is associated with low D2-receptor density in the ventral striatum (Dalley et al. 2007). Moreover, trait impulsivity has been shown to promote the transition of control of reward-seeking behavior from ventral to dorsal striatal regions (Belin and Everitt 2008; Belin et al. 2008). On the basis of this literature, we predict that administration of D2-receptor drugs to healthy volunteers will alter the influence of the ventral striatum on the dorsal putamen, through the dorsal caudate nucleus, in a manner that depends on trait impulsivity. Following prior work (Cools et al. 2007; Dalley et al. 2007; Clatworthy et al. 2009), we hypothesize that dopaminergic drugs would have greater effects in high-impulsive subjects (with putatively low D2-receptor density) than in low-impulsive subjects.

We employed a 2 × 2 factorial pharmacological design and manipulated dopamine receptor stimulation in a group of healthy participants by administration of a dopamine D2-receptor agonist (bromocriptine), a dopamine D2-receptor antagonist (sulpiride), a combination of the agonist and antagonist, and a placebo, in a four-session, within-subject, double-dummy, placebo-controlled cross-over design. This factorial pharmacological design allowed us to assess the neurochemical specificity of effects. If any effects of the D2-receptor agonist bromocriptine depend on dopamine's action on D2-receptors, then they should be blocked by pretreatment with sulpiride.

Blood oxygenation level-dependent (BOLD) signal was measured using functional magnetic resonance imaging (fMRI) during rest. This approach allowed us to relate task-independent features of intrinsic striatal connectivity to trait-related individual differences in mesostriatal dopamine systems. We used stochastic dynamic causal modeling (DCM; Friston et al. 2011; Li et al. 2011; Daunizeau et al. 2012) to model interactions between motivational, cognitive, and motor portions of the striatum and their modulation by dopamine. This method estimates the extent to which fluctuations in activity of one region cause fluctuations in another region. The results demonstrate that dopamine modulates intrastriatal connectivity and that the degree of dopaminergic modulation of dorsomedial striatum (dorsal caudate nucleus) by ventral striatum is associated with trait impulsivity.

Materials and Methods

Participants

Twenty-eight participants gave informed consent approved by the local ethical committee ("Commissie Mensgebonden Onderzoek," Arnhem-Nijmegen, number: 2008/078). Three participants were excluded from the analysis: 2 participants withdrew before completing all 4 sessions; one dataset was unusable due to a technical problem. The 25 participants included in the analysis were right-handed (13 women; mean age 22 years, range 18–30 years), with no relevant medical or psychiatric condition 3 years prior to testing.

Factorial Pharmacological Design

We employed a 2 × 2 factorial pharmacological design (Table 1). The 2 pharmacological factors were bromocriptine, a dopamine receptor agonist, and sulpiride, a dopamine receptor antagonist. Each of these factors could be "ON" (drug) or "OFF" (placebo). Each participant was tested on each cell of this factorial design, receiving 2 different opaque gelatin capsules on 2 separate time points on each of the 4 testing sessions, corresponding to these 2 pharmacological factors (double-dummy design). Thus, 2 pharmacological factors could affect mesostriatal system: Whether sulpiride was ON or OFF, and whether bromocriptine was ON or OFF. This design allowed us to quantify not only the main effects of sulpiride and bromocriptine, but also their interaction effect. If the effects of bromocriptine are mediated by dopaminergic D2-receptors, those should be abolished by co-administration with sulpiride.

The dose selection of sulpiride (Dogmatil®, Sanofi-aventis, 400 mg) and bromocriptine (Parlodel®, Novartis, 1.25 mg) was based on previous studies revealing good tolerance (Mehta et al. 2004; Cools et al. 2009; Dodds et al. 2009). Participants received the capsule corresponding to the bromocriptine factor 30 min after receiving the one corresponding to the sulpiride factor. The order of drug administration was pseudorandomly assigned and counterbalanced across participants. The resting-state fMRI started approximately 2 h after first drug intake and took 7.5 min. Participants were instructed to relax and keep their eyes open. The resting-state fMRI data reported here were acquired prior to the acquisition of a task-related fMRI session, during which participants completed a reversal learning task reported in van der Schaaf et al. (2014).

The mean time to maximal plasma concentration of sulpiride and bromocriptine is approximately 3 and 2.5 h, respectively, with a plasma half-life of approximately 12 and 7 h, respectively (Deleu et al. 2002; Mehta et al. 2004). Accordingly, drug had maximum effects during testing. Subjective mood ratings were measured with the Bond and Lader visual analog scales (Bond and Lader 1974). Mood measures, blood pressure, and heart rate were taken approximately 30 min before, approximately 2 h after, and approximately 6 h after first drug intake [reported in van der Schaaf et al. (2014)]. Participants' general cognitive performance and mood were not different following different drug sessions, indicating that effects were not due to nonspecific drug effects on mood and global cognitive performance.

Image Acquisition and Preprocessing

Structural [T_1-weighted magnetization prepared rapid gradient echo sequence, time echo/time repetition (TE/TR) = 3.03/2300 ms,

Table 1 Factorial pharmacological design

Session name	Placebo	Bromocriptine	Sulpiride	Combined
Factor 1 (Bromocriptine)	OFF	ON	OFF	ON
Factor 2 (Sulpiride)	OFF	OFF	ON	ON

Note: We employed a 2 × 2 factorial pharmacological design, where pharmacological factors were bromocriptine, a dopamine receptor agonist, and sulpiride, a dopamine receptor antagonist. Each of these factors could be "ON" (drug) or "OFF" (placebo).

flip angle = 8°, field of view (FOV) = 256 × 256 × 192 mm, voxel size = 1 mm isotropic, generalized autocalibrating partially parallel acquisition (GRAPPA) acceleration factor 2] and functional images (whole-brain gradient-echo planar imaging sequence; TE/TR = 30/1680 ms, flip angle = 70°, FOV = 224 × 224 × 137 mm, 39 ascending transverse slices; voxel size = 3.5 × 3.5 × 3.0 mm) were collected using a 3-T Siemens MRI scanner with an 8-channel head coil. To reduce signal drop-out and geometric distortions, we used a short TE and reduced echo train length by means of accelerated GRAPPA (Griswold et al. 2002).

Images were preprocessed using SPM8 (Wellcome Trust Center for Neuroimaging, London, UK) and MATLAB. The images were realigned, slice-time corrected, and coregistered to the structural image. Participants' head motion during fMRI acquisition did not differ between experimental sessions, as indexed by the session-specific average head translation and tested with a 2-by-2 full-factorial ANOVA (factors: sulpiride and bromocriptine; all $P > 0.05$). The images were then smoothed with an isotropic 5-mm full-width half maximum Gaussian kernel. Images were low-pass filtered using a fifth order Butterworth filter to retain frequencies below 0.1 Hz, because the correlations between intrinsic fluctuations are specific to this frequency range (Biswal et al. 1995; Fox and Raichle 2007). The images were also high-pass filtered (0.008 Hz) to remove low-frequency confounds. To remove nonneuronal fluctuations from the data, we regressed out 27 regressors from each time series: 3 regressors describing time series of average signal intensity in white matter, cerebro-spinal fluid, and in a blank portion of the MR images (out of brain signal; Helmich et al. 2010); 24 regressors describing time series of head motion, namely linear and quadratic effects of the 6 parameters describing the motion of each fMRI image, as well as the first derivative of those effects (to control for spin-history effects; Lund et al. 2005).

The striatal data were extracted using a striatal mask based on the Harvard-Oxford atlas (Flitney et al. 2007). Nonneuronal fluctuations that might be introduced to the data due to individual differences in the striatal size were further controlled using linear regression. Thus, for each subject, we considered the first principal component across voxels within the striatal mask that fell into either white matter or cerebro-spinal fluid (with probability >0.99) and regressed out that signal, its square and its cube from all striatal voxels signal.

Functional Parcellation of the Striatum

To ensure a functionally informed parcellation of the striatum, we based our segregation on the functional time series, using clustering analysis of the correlations among voxel time series. Furthermore, to ensure that this parcellation scheme was valid at the between-subject level, we performed a stability analysis to identify clusters that were conserved over subjects. We used K-means clustering algorithm to identify different subdivisions of the striatum. In this algorithm, those voxels with higher similarity in correlation pattern of their time series are more likely to be clustered together. The correlation pattern of each voxel in the striatum was quantified based on its correlation with all other striatal voxels. Therefore, first the correlation matrix for each participant was computed using correlation between each striatal voxel with all other striatal voxels. Next, to compute correlation matrix across group, the individual correlation matrices were Fisher-transformed, averaged, and transformed back to correlation space by inverse Fisher transform. We then used a standard K-means clustering algorithm, using correlation as a distance measure, as implemented in MATLAB *kmeans* routine (Mathwork) to parcellate the striatum. Each clustering analysis was replicated 20 times with random initial centroids to avoid local extrema.

K-means clustering operates on a user-defined number of clusters. Since this number is unknown, we performed a stability analysis to identify the most consistent and coherent number of clusters. Subjects were randomly divided into 2 groups and a series of parcellation into 2–8 clusters was carried out separately for each group. The clustering solutions based on data of 2 groups were then assessed to examine whether they are matched (see Appendix for mathematical definition). This procedure was repeated for 100 randomly division of subjects to 2 groups and used to perform a Monte Carlo randomization test to obtain the largest K resulting in stable clustering solution across group.

This analysis ensures us that this parcellation scheme was valid across the group and results in clusters that could be reliably identified over group. It is important to realize that the goal of functional parcellation and the stability analysis were not to determine the number of striatal subregions. Rather, the goal of this stability analysis is to find subregions that (1) are consistent at the group level given limitations of fMRI signals and (2) have a distinct pattern of connectivity from the point of view of data (Neubert et al. 2014).

Having established K, we again performed clustering to define the striatal clusters. For every participant and every session, the clustering algorithm defined 5 clusters according to striatal connectivity matrix of all other remaining subjects in the same session (leave-one-subject-out procedure). The clusters were matched very closely across different sessions and across the 25 cross-validation folds. The leave-one-subject-out procedure ensures that there is no selection bias in definition of regions of interest.

Following classical models of the striatum and to limit model space for DCM analysis, we considered a 3-nodes architecture for the striatum. Thus, the ventral striatum, dorsal caudate nucleus, and dorsal-anterior putamen clusters out of the clustering solution with $K = 5$ were then chosen as representative of motivational, cognitive, and premotor striatum, respectively. For each participant, the spatial intersection of these 3 clusters across 4 sessions was generated and used as volume of interests. The first eigenvariate of data in each volume of interest was then extracted for every session.

Dynamic Causal Modeling

We used DCM software implemented in SPM12b (version: 5616). All models were inverted using generalized filtering (Friston et al. 2010; Li et al. 2011) successfully. The inversion scheme estimated model evidence and fixed connections and dopaminergic-modulatory parameters (as well as hemodynamic parameters) for each model. The estimated model evidence reflects the plausibility of the model taking into account both goodness of fit and model complexity. We used random-effects Bayesian model comparison to evaluate the plausibility of every model of the model space across the population (Stephan et al. 2009) and report the results in terms of protected exceedance probabilities (Rigoux et al. 2014) throughout the study.

Results

Resting-state data were analyzed from 25 healthy volunteers who participated in a fMRI experiment, in which both resting-state as well as task-related data were collected (van der Schaaf et al. 2014). We employed a 2 × 2 factorial pharmacological design (Table 1). Therefore, each participant was tested on each cell of this factorial design, receiving 2 different opaque gelatin capsules

on each of the 4 testing sessions, corresponding to the combinations of the 2 pharmacological factors. Trait impulsivity was indexed with the Barratt Impulsiveness Scale (BIS; Patton et al. 1995; see Supplementary Table 1). Previous work with [^{11}C]raclopride positron emission tomography (PET) in healthy volunteers has shown that subjects with high BIS scores exhibit lower D2-receptor availability than do subjects with low BIS scores (Buckholtz et al. 2010). Moreover, BIS scores have been shown to predict the direction of bromocriptine's effects on striatal BOLD signal (Cools et al. 2007). The BIS was administered in each session approximately 5.5 h after first drug intake. The average of the BIS scores across all 4 sessions was used as an index of trait impulsivity (For one subject, BIS scores were obtained only in 2 out of the 4 sessions. For this subject, the average across these 2 sessions was used), given the high intersession correlation between those scores (all pair-wise correlations >0.9), and the absence of significant drug effects on total BIS scores ($P > 0.05$ for main effects and interaction, controlled for order effect).

Defining Motivational, Cognitive, and Motor Striatal Nodes

There are no reliable in vivo structural markers of the boundaries between functionally distinct regions of the human striatum (Voorn et al. 2004), namely the motivational, cognitive, and motor regions. Here, we overcome this obstacle by using an unsupervised parcellation scheme based on correlation between functional time series. The parcellation scheme identified 5 clusters reliably at the population level ($P < 0.05$, Monte Carlo randomization test, see Materials and Methods and Appendix for description, Supplementary Fig. 1A). The clustering solution included a ventral striatal region (including nucleus accumbens, ventral caudate nucleus, and ventral parts of the putamen), a medial caudate region, a dorsal caudate nucleus region, a dorsal-anterior putamen region, and a dorsal-posterior putamen region (Supplementary Fig. 1B). The macroanatomical borders of these clusters were consistent with connectivity pattern of the striatum measured with various techniques in different species (Haber et al. 2000; Ikemoto 2007; Draganski et al. 2008). Although the clustering algorithm was blind to voxel location, there was a very high symmetry between 2 hemispheres as >95% of symmetric voxels assigned to the same clusters.

Following classical models of the striatum based on hypothesized functions of striatal regions and its cortical connectivity signature (Alexander et al. 1986; Haber et al. 2000) and to limit model space for DCM analysis, we considered a 3-nodes architecture for the striatum. Thus, the ventral striatum, dorsal caudate nucleus, and dorsal-anterior putamen cluster were chosen as representative of motivational, cognitive, and premotor striatum, respectively (Fig. 1A). We focused on the dorsal caudate nucleus, given its strong associations with cognitive control and associated cortical regions (e.g., the dorsolateral prefrontal cortex; Haber et al. 2000; Draganski et al. 2008). We focused on the dorsal-anterior putamen, because it is known to be a target of dopaminergic-mediated connectivity from the dorsal caudate nucleus (Haber et al. 2000), while being strongly associated with premotor cortex (e.g., the rostral cingulate motor areas) as well as lateral prefrontal cortex (Calzavara et al. 2007; Draganski et al. 2008; Helmich et al. 2010). Note that although the rostral cingulate motor area is implicated in premotor functions [e.g., by sending direct projections to the spinal cord (He et al. 1995) and primary motor cortex (Dum and Strick 2002)], this area is also associated with negative affect, pain, and cognitive control (Shackman et al. 2011).

For each participant, the spatial intersection of these 3 clusters across 4 sessions was generated and used as volume of interests. The first eigenvariate of data in each volume of interest was then extracted for every session.

Dopaminergic Drug Effects on Intrastriatal Effective Connectivity

We constructed stochastic DCMs to assess dopaminergic drug effects on intrastriatal connectivity using the first eigenvariate of each of the 3 striatal regions as a summary time series, after removal of nuisance-related variance.

DCM enjoys a property of Bayesian schemes, namely the ability to dissociate between the goodness of a particular model architecture based on the data, and the consistency (nonzero) of experimental effects on the model parameters across the population. This property is important for the purpose of this study, given that dopaminergic drug effects on the striatum likely vary widely across participants (Cools and D'Esposito 2011). Accordingly, across the whole group, the dopaminergic drug effects across the group as a whole on intrastriatal connectivity might average around zero. Yet, by using DCM, we could assess the degree to which the drug alters intrastriatal connectivity even when the sign of this effect differs across participants. Specifically, we included dopaminergic drugs as modulatory pharmacological inputs (PIs) in DCM, and then used Bayesian model comparison to assess effects of sulpiride and bromocriptine across the group, independent of the sign of their effects between individuals.

Model Space

Our model space had 3 factors. These included the nature of the drug effects (i.e., the PIs, see Fig. 1*B*), the underlying intrastriatal connectivity architecture (Fig. 1*C*), and the modulation of these intrastriatal connections by dopamine (Fig. 1*D*). The first factor concerned the effects of the pharmacological manipulation, modeled as extrinsic modulatory PI, enabling us to assess both the main and interaction effects of our 2 pharmacological factors sulpiride and bromocriptine. This resulted in 5 sets of PI (PI1–PI5 in Fig. 1*B*). The second factor concerned the presence of directed connections among the 3 striatal nodes, yielding in total 5 types of hypothetical striatal architecture (A1–A5 in Fig. 1C). Finally, the effects of dopamine on these 5 types of intrastriatal architecture were investigated by allowing pharmacological (dopaminergic) inputs to modulate the intrastriatal architectures in 5 different ways (B1–B5 in Fig. 1*D*), in addition to a null model with no modulation (B0 in Fig. 1*D*). It should be noted that our model space did not include models in which dopamine was allowed to modulate nonexistent connections, as this was considered biologically implausible (e.g., A1B2). In total, we considered 15 different mesostriatal architectures (see the list in Fig. 1*F*). Here, 5 models were null models with no modulation but with different underlying architectures (i.e., the B0 models). The combination of the other 10 mesostriatal architectures (B1–B5) with the 5 sets of PIs (PI1–PI5) resulted in a total of 50 models. Together with the 5 null models, this resulted in a final model space of 55 models.

The first factor concerned different scenarios of the effects of pharmacological drugs: (1) A main effect of bromocriptine, but no effect of sulpiride. In this model, bromocriptine, but not sulpiride, was allowed to change striatal connectivity (Fig. 1*B*, PI1); (2) a main effect of sulpiride, but no effect of bromocriptine. In this model, sulpiride, but not bromocriptine, was allowed to change striatal connectivity (Fig. 1*B*, PI2); (3) a main effect of sulpiride, a main effect of bromocriptine, and no interaction between

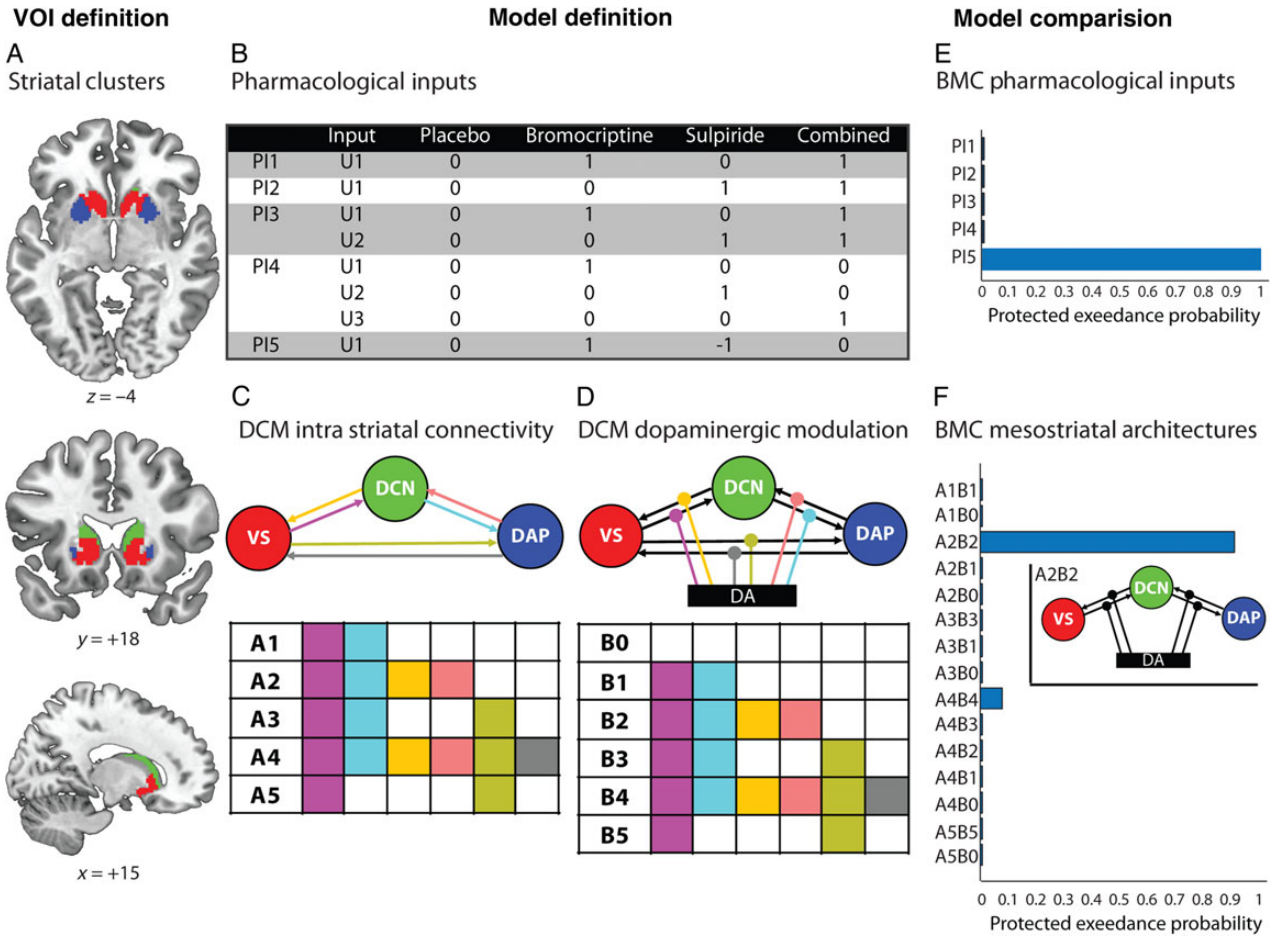

Figure 1. VOI definition, model definition, and model selection. (*A*) Striatal clusters obtained using data-driven parcellation of the human striatum in motivational (VS in red), cognitive (DCN in green), and motor (DAP in blue) regions. (*B*) Model space of PI, representing different scenarios for the effects of sulpiride and bromocriptine. Dopaminergic drugs have been included as extrinsic modulatory PIs. These scenarios differ in how they might capture the effects of bromocriptine and sulpiride, namely as only an effect of bromocriptine (PI1) or only an effect of sulpiride (PI2), independent effects of both (PI3), independent effects of both but a potentially nonlinear (and independently estimated) effect of combined administration (PI4), or antagonistic and symmetric effects of both (PI5). Thus, the number of inputs varies across the different sets of PIs. For example, whereas PI4 contains 3 inputs (U1, U2, and U3), PI5 contains only 1 input (U1). In PI5, the only input, U1, is +1 in the bromocriptine session, −1 in the sulpiride session, and 0 in the placebo and combined session. Therefore, this pharmacological input refers to a situation in which bromocriptine and sulpiride show opponent and symmetric effects, such that coadministration of bromocriptine with sulpiride abolishes the effects evoked when administered alone. (*C*) Models of intrastriatal connectivity that differed in terms of the number and directionality of the connections between the 3 striatal regions (A-matrix). Colors are associated with different intrastriatal connections. The table highlights which connections are included in each model. For example, A2 includes 4 connections represented with different colors: magenta (VS → DCN), cyan (DCN → DAP), yellow (DCN → VS), and salmon (DAP → DCN). (*D*) Models of dopaminergic-modulatory effects on striatal connections. Colors are associated with different dopaminergic-modulatory connections (B-matrix). The table in this panel shows which modulatory connections are included in each model. The combination of the A-matrix and the B-matrix resulted in 15 hypothetical mesostriatal architectures (listed in Fig. 1F *y*-axis). For example, for A2, 3 models of dopaminergic modulation are possible: A2B2, A2B1, and A2B0. In A2B2, there are 4 modulatory connections represented with different colors: magenta (modulating VS → DCN), cyan (modulating DCN → DAP), yellow (modulating DCN → VS), and salmon (modulating DAP → DCN). In A2B1, whereas A2 contains 4 links, there are only 2 modulatory connections in B1: magenta (modulating VS → DCN) and cyan (modulating DCN → DAP). A2B0 is a null model where there is no modulatory effect of dopamine, as shown in the table for B0. (*E*) Random-effects family Bayesian model comparison results for pharmacological input. The pharmacological input with symmetric effects of sulpiride and bromocriptine (PI5) best matches the fMRI data, suggesting that sulpiride and bromocriptine affects striatal connectivity to the same degree, but in opposite directions and with any possible asymmetric effects of sulpiride and bromocriptine being negligible. The *x*-axis represents the protected exeedance probability. (*F*) Random-effects Bayesian model comparison for 15 mesostriatal architectures with PI5 as the pharmacological input [models with no modulatory inputs (B0) were also included]. The model with forward and backward projections between the VS and the DCN as well as between the DCN and the DAP, A2B2, is the most plausible model across the population. The *x*-axis is the protected exeedance probability. Inset: The winning mesostriatal architecture, A2B2. VOI, volume of interest; PI, pharmacological input; DCM, dynamic causal modeling; VS, ventral striatum; DCN, dorsal caudate nucleus, DAP, dorsal-anterior putamen; DA, dopamine; BMC, Bayesian model comparison.

sulpiride and bromocriptine. In this model, both sulpiride and bromocriptine were allowed to change the striatal connectivity independently, and the effect of the combined session corresponded to the sum of their effect when administered alone (Fig. 1B, PI3); (4) a main effect of sulpiride, a main effect of bromocriptine, and an interaction effect of sulpiride and bromocriptine. In this model, both sulpiride and bromocriptine were allowed to change striatal connectivity independently, as well as their interaction. Namely, in the combined session, the effects of sulpiride and bromocriptine could vary independently of their effects when administered alone (Fig. 1B, PI4). (5) Symmetric effects of sulpiride and bromocriptine on striatal connectivity (Fig. 1B, PI5). In this model, the magnitude of the effect of bromocriptine was equal to that of sulpiride, but in the opposite direction.

The second factor concerned intrastriatal connections, independently from the dopaminergic modulations (Fig. 1C). We created 4 models containing forward connections from the ventral striatum to the dorsal caudate nucleus; and from the dorsal caudate nucleus to the dorsal-anterior putamen. This feature of the models is grounded in neuroanatomical evidence from non-human primates that demonstrate the presence of forward information flow along the mediolateral gradient across the striatum (Haber et al. 2000). This property, as well as contribution of backwards connections, was assessed by constructing 4 intrastriatal architectures: (1) A forward connection from the ventral striatum to the dorsal caudate nucleus and from the dorsal caudate nucleus to the dorsal-anterior putamen (Fig. 1C, A1); (2) both forward and backward connections between the ventral striatum and the dorsal caudate nucleus and between the dorsal caudate nucleus and the dorsal-anterior putamen (Fig. 1C, A2); (3) forward connections from the ventral striatum to the dorsal caudate nucleus, from the dorsal caudate nucleus to the dorsal-anterior putamen and from the ventral striatum to the dorsal-anterior putamen (Fig. 1C, A3); (4) forward and backward connections between all 3 subregions (Fig. 1C, A4). Finally, we included a model with (5) 2 connections, one from the ventral striatum to the dorsal caudate nucleus and the other one from the ventral striatum to the dorsal-anterior putamen. This model was created based on data, showing that the ventral striatum sends trisynaptic projections to the primary motor cortex and to prefrontal cortex (Kelly and Strick 2004), which could result in modulation of the dorsal caudate nucleus and the dorsal-anterior putamen by modulating their associated cortical areas in the cognitive and motor loops of frontostriatal circuitry.

The third factor concerned the effects of dopamine on intrastriatal connectivity. We constructed models that allowed modulatory effects of dopamine on all (Fig. 1D, B4), some (Fig. 1D, B1, B2, B3, and B5), or none (Fig. 1D, B0) of the striatal architectures described above. The effects of sulpiride and bromocriptine were assumed to be homogeneous with respect to input type, across the different striatal connections.

Hypotheses

On the basis of this neuroanatomical and neurochemical evidence (Haber et al. 2000; Ikeda et al. 2013), we hypothesized that dopaminergic drugs would modulate the flow of information in a directional forward fashion along the mediolateral gradient in the striatum. Furthermore, previous PET work has shown that impulsivity-dependent dopaminergic effects are mediated by the D2-receptor (Dalley et al. 2007; Buckholtz et al. 2010). Accordingly, we anticipated that our data would be best fit by model A1B1 and that individual differences in dopaminergic drug effects, as indexed by the modulatory B parameters, would depend on trait impulsivity. To test this hypothesis, we assessed not only the effects of the D2-receptor agonist bromocriptine, which also has affinity for the D1-receptor (while also altering noradrenalin transmission), but also the effects of sulpiride, a highly selective antagonist for the D2-receptor. In addition, we assessed in a combined session whether the effects of bromocriptine would be blocked by pretreatment of sulpiride. We predicted that the effect of bromocriptine would be opposite to that of sulpiride, and that these would not interact. If the effect of bromocriptine would be equal in size to that of sulpiride, then the combined administration would be indistinguishable from that of placebo. In this case, the data would be best fit by input set PI5. However, if the effects of bromocriptine and sulpiride are independent but of unequal size, then the data would be best fit by input set PI3.

Model Selection

We employed a two-step model selection approach. First, we performed a family-wise random-effects Bayesian model comparison to test the pharmacological drug effects (Fig. 1E; Penny et al. 2010). Second, we performed a random-effects Bayesian model comparison to compare different mesostriatal architectures given the winner input in the previous step (Fig. 1F; Rigoux et al. 2014).

First, Bayesian model comparison over the model space of PI revealed very strong evidence in favor of the PI family with opponent, symmetric effects of sulpiride and bromocriptine (PI5, protected exceedance probability of 1.00, expected posterior model probability of 0.50; Fig. 1E). Thus, sulpiride and bromocriptine altered intrastriatal connectivity to the same degree, but in opposite directions, consistent with the hypothesis that dopaminergic drug effects on mesostriatal connectivity are mediated by the D2-receptor. In this winning model, the effects of sulpiride and bromocriptine on intrastriatal coupling cancelled each other out, leaving a zero net effect.

Second, Bayesian model comparison over the model space of mesostriatal architectures revealed evidence in favor of the architecture with forward and backward projections between the ventral striatum and the dorsal caudate nucleus as well as between the dorsal caudate nucleus and the dorsal-anterior putamen (A2B2, protected exceedance probability of 0.92, expected posterior model probability of 0.40; Fig. 1F). In summary, the winning model contains bidirectional connections between striatal regions, in a hierarchical fashion, and a modulatory input on each of these connections to model the opponent dopaminergic drug effects.

These results were robust to model selection procedures: A one-step random-effects Bayesian model comparison among all 55 models revealed that the same model, A2B2, best explained our data across the whole model space (protected exceedance probability of 0.95, expected posterior model probability of 0.19).

Trait Impulsivity and Dopaminergic Drug Effects on Intrastriatal Effective Connectivity

Further analysis of the characteristics of the winning model led to an important additional insight on how dopamine modulates intrastriatal connectivity. First, using one-sample *t*-tests, we confirmed that each of the 4 parameters quantifying intrastriatal connectivity in the winning model was significantly above zero (all $P < 0.006$, Bonferroni-corrected, Supplementary Table 2). This observation is consistent with the expectation that the 3 striatal subregions are strongly connected. Second, the same statistical procedure revealed that none of the 4 parameters quantifying dopaminergic modulation of intrastriatal connectivity was significantly different from zero (all $P > 0.006$, Bonferroni-corrected, Supplementary Table 2). This null-effect persisted even when the statistical threshold was relaxed to 0.05 uncorrected for multiple comparisons (see Supplementary Table 2). This null-effect might seem to contradict the model selection results. In fact, these observations indicate that dopaminergic-modulatory inputs explain significant variance in the fMRI time series, despite the fact that the "sign" of the modulatory effect is inconsistent across subjects. The latter finding fits with the known interindividual variability in the direction and extent of dopaminergic drug effects (Cools and D'Esposito 2011). Strong dopaminergic drug effects in individual participants often add to zero when averaged across a group (Cools and D'Esposito 2011). Given that individual differences in dopaminergic drug effects on striatal activity have been shown to depend on trait

impulsivity according to D2-receptor density (Cools et al. 2007; Dalley et al. 2007), we hypothesized that effects of D2-receptor agents on intrastriatal connectivity are associated with trait impulsivity. Therefore, we tested whether modulatory input parameters of the winning model are associated with trait impulsivity. This analysis was implemented through a repeated-measures ANOVA, assessing individual modulatory parameters as a function of connection direction (forward vs. backward), striatal pair (ventral striatum–dorsal caudate nucleus or dorsal caudate nucleus–dorsal-anterior putamen), and trait impulsivity (BIS scores). This analysis revealed a significant positive association between impulsivity and connection strength ($F_{1,23} = 4.52$, $P = 0.044$). Crucially, there was a significant three-way interaction between trait impulsivity, striatal pair, and connection direction ($F_{1,23} = 4.71$, $P = 0.041$). Post hoc correlation analyses revealed that the three-way interaction was due to a highly significant positive correlation between trait impulsivity and the drug effects on the forward connection from the ventral striatum to the dorsal caudate nucleus ($r = 0.53$, $P = 0.007$, Fig. 2B). Trait impulsivity did not correlate with drug effects on the other connections ($P > 0.05$, Supplementary Table 3). These results indicate that trait impulsivity is associated with the increasing and decreasing effects of, respectively, bromocriptine and sulpiride on the forward connection from the ventral striatum to the dorsal caudate nucleus, but not on the other connections. Thus, trait impulsivity is associated with an increased dorsal caudate nucleus drive from the ventral striatum by stimulation of D2-receptors, and a decreased dorsal caudate nucleus drive from the ventral striatum by blockade of D2-receptors.

We also performed 2 control analyses regarding the association of impulsivity with connectivity between the ventral striatum and the dorsal caudate nucleus. First, we conducted a control analysis using BIS scores in the placebo session, instead of the original analysis with mean across all 4 sessions, as the index of trait impulsivity. The results of this control analysis were consistent with those of main analysis (see Supplementary Material). Second, we conducted a relatively model-free analysis (linear regression) to confirm our findings regarding the association of impulsivity with the connectivity between the ventral striatum and the dorsal caudate nucleus, independent of the estimated effective connectivity strengths in the winning mesostriatal architecture from DCM (see Supplementary Material). The results of this analysis were consistent with those found based on DCM (Supplementary Fig. 2 and Table 4).

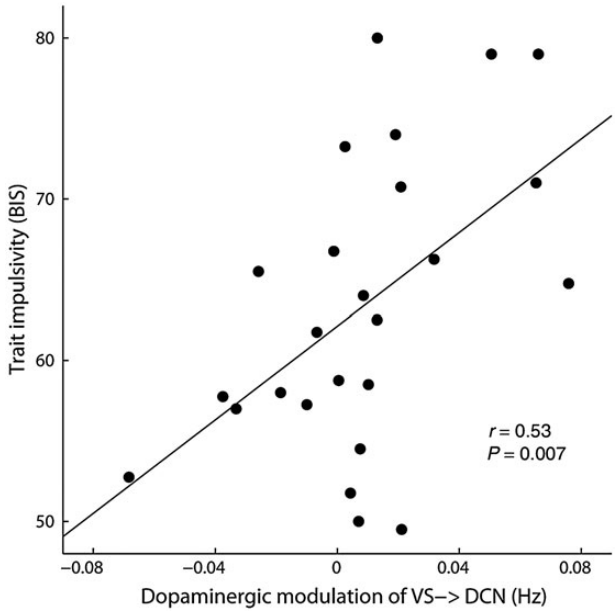

Figure 2. The relationship between dopaminergic modulation of striatal ventrodorsal connectivity and trait impulsivity. Scatter plot shows the relationship between trait impulsivity and the modulatory parameter encoding dopaminergic modulation of the connection from the ventral striatum to the dorsal caudate nucleus in the winning model. Trait impulsivity is associated with drug-induced increases (decreases) by D2 dopamine agonist (D2 dopamine antagonist) of dorsal caudate nucleus input from VS. BIS, Barratt impulsiveness scale; VS, ventral striatum; DCN, dorsal caudate nucleus; Hz, Hertz.

Dopamine-Mediated Connectivity of Dorsal-Posterior Putamen

It is known that selection of the best model among a large number of competing hypotheses could be fragile, especially if the data of different subjects could be fitted by different models (as could happen in a random-effect model space; Penny et al. 2010). Therefore, we have tested our a priori hypotheses on striatal connectivity on models comprising 3 nodes. This approach generates robust inferences, but it also limits the inference of the study to ventral and dorsal-anterior portions of the striatum. Here, following a reviewer's comment, we build on those findings and extend the analysis to a more posterior part of the striatum.

Connectivity-based parcellation of the striatum identified a dorsal-posterior putamen cluster (Fig. 3A), known to be connected to motor cortex and strongly implicated in motor control (Draganski et al. 2008; Helmich et al. 2010) and habitual action selection (Wunderlich et al. 2012). Neuroanatomical evidence in nonhuman primates (Haber et al. 2000) suggests that dopamine modulates forward connections along the mediolateral gradient across the striatum. Therefore, we extended the intrastriatal architecture by adding "forward" connection from the dorsal-anterior putamen to the dorsal-posterior putamen (Fig. 3B, a1). Two models of dopaminergic modulation associated with this architecture were tested, where dopamine either modulated or did not modulate this connection (Fig. 3B, b1 and b0, respectively). A second intrastriatal architecture was created by including "bidirectional" connections between the dorsal-anterior putamen and the dorsal-posterior putamen. Three models of dopaminergic modulation associated with this architecture were tested, where dopamine modulated none (Fig. 3B, b0), the forward connection (Fig. 3B, b1), or both connections (Fig. 3B, b2) from the dorsal-anterior putamen to the dorsal-posterior putamen. Finally, we included a third intrastriatal architecture where the ventral striatum directly modulated the dorsal-posterior putamen (Fig. 3B, a3). This model was created based on data, showing that the ventral striatum sends trisynaptic projections to the primary motor cortex and to the prefrontal cortex (Kelly and Strick 2004), which could result in a ventral striatal modulation of dorsal-posterior putamen through the motor loop of the frontostriatal circuitry. Two models of dopaminergic modulation associated with this architecture were tested, where dopamine either modulated (Fig. 3B, b3) or did not modulate this connection (Fig. 3B, b0).

These models were fitted and compared using random-effects Bayesian model comparison. This analysis revealed strong evidence in favor of the mesostriatal architecture with forward and backward baseline connections between the dorsal-anterior putamen and the dorsal-posterior putamen, where dopamine modulated both connections (Fig. 3C, protected exceedance probability of 1.00, expected posterior model probability of 0.81). These findings extend our prior findings to more posterior parts

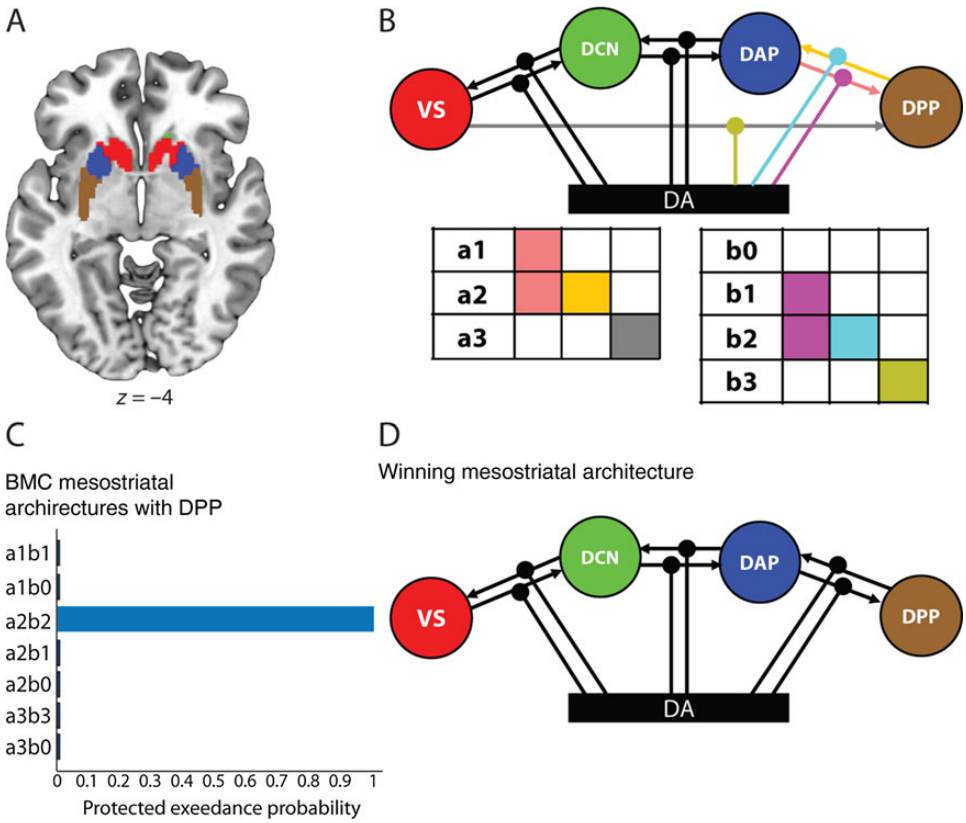

Figure 3. Post hoc analysis of dopamine-mediated connectivity of DPP. (*A*) DPP cluster (in brown) obtained using data-driven parcellation of the human striatum. (*B*) Three models of intrastriatal connectivity of DPP and 4 models of its dopaminergic modulation were created. The table highlights which connections are included in each model. In total, 7 models were tested. Note that the pharmacological input as well as mesostriatal connections among other striatal regions are fixed according to the optimal model presented in Figure 2. (*C*) Random-effects Bayesian model comparison for 7 mesostriatal architectures with DPP. Bayesian model comparison strongly favored a2b2 among all 7 models. (*D*) The winning mesostriatal architecture. Striatal areas are bidirectionally connected along a mediolateral gradient and dopamine modulates adjacent areas along this gradient. VS, ventral striatum; DCN, dorsal caudate nucleus; DAP, dorsal-anterior putamen; DPP, dorsal-posterior putamen; DA, dopamine; BMC, Bayesian model comparison.

of the striatum. The findings suggest that dopamine modulates both forward and backward intrastriatal connections along the mediolateral axis of the striatum (Fig. 3*D*).

Discussion

This pharmacological fMRI study addresses the functional architecture of the human striatum and dopaminergic influences on striatal information processing (Cools et al. 2007; Dalley et al. 2007; Belin et al. 2008). We manipulated the connectivity between motivational, cognitive, and motor portions of the striatum with dopaminergic drugs, and we exploited interindividual differences in mesostriatal dopamine systems to explain trait-dependent effects of the dopaminergic manipulations. Striatal connectivity patterns were quantified with stochastic DCM of intrinsic BOLD activity measured in a within-subject, double-dummy, placebo-controlled cross-over design. There are 2 main findings. First, Bayesian model comparison indicates that human striatal architecture is sparse and largely consistent with neuroanatomical data from nonhuman primates and rodents (Haber et al. 2000). Namely, functional interactions between the ventral striatum and the dorsal-anterior putamen are mediated by the dorsal caudate nucleus, and the efficacy of those interactions is modulated by dopaminergic tone. Second, the magnitude of the dopaminergic modulation of a portion of those interactions depends on trait impulsivity. Namely, highly impulsive individuals have increased sensitivity to dopamine-induced changes in information flow from the ventral to the dorsomedial striatum. This result might explain how, in highly impulsive individuals, cognitive processes supported by the dorsomedial striatum can become particularly vulnerable to the motivational drive from the ventral striatum (Lawrence and Brooks 2014).

Intrinsic Striatal Architecture

This study shows that a model of striatal connectivity without a direct connection between the ventral striatum and the dorsal-anterior putamen fitted the data significantly better than models with such a connection. This finding suggests that communication between those 2 striatal regions is mediated by the dorsal caudate nucleus. In macaques, dopamine mediates information flow along the mediolateral pathway through serial reciprocal connections between the striatum and the midbrain (Haber et al. 2000). Accordingly, we interpret the effects of stimulation and blockade of D2-receptors at the level of the striatum in terms of altered midbrain-mediated feedforward information flow from the ventral striatum to the dorsal caudate nucleus. However, we cannot exclude concurrent actions via modulation of topographically specific, feedforward circuits connecting the prefrontal cortex with the striatum (McFarland and Haber 2002; Honey et al. 2003; Haber and Knutson 2010; Cole, Beckmann, et al. 2013; Cole, Oei, et al. 2013).

Impulsivity Amplifies Dopaminergic Modulations of Ventrodorsal Striatal Connectivity

Work with behaving rodents indicates that the transition from impulsive to compulsive drug use, and the corresponding transition of behavioral control from the ventral to the dorsolateral striatum, can be promoted by dopamine (Dalley et al. 2007; Belin and Everitt 2008; Belin et al. 2008). Dalley et al. (2007) have shown that ventral striatal D2-receptors density predicts individual difference in trait impulsivity, which itself predict propensity to cocaine seeking (Dalley et al. 2007) and addiction-like behavior (Belin et al. 2008). Our findings add to this body of knowledge by showing that trait impulsivity is associated with the influences of striatal D2-receptors on how effectively the ventral striatum modulates activity in the dorsal caudate nucleus. This effect was specific: The dopaminergic drugs were found to modulate connectivity along both the ventral striatum to the dorsal caudate nucleus and the dorsal caudate nucleus to the dorsal-anterior putamen pathway, whereas impulsivity was associated with only the first part of that pathway. Work with experimental animals (Dalley et al. 2011) raises the intriguing possibility that compulsivity might convey vulnerability of the connection between the dorsomedial and dorsolateral striatum to dopaminergic drugs.

Limitations

It can be argued that the current findings are statistical constructs of an oversimplified model of intrinsic striatal connectivity. In fact, stochastic DCM provides an objective and quantitative procedure for distinguishing between explicit models of functional anatomy (Friston et al. 2011; Li et al. 2011; Daunizeau et al. 2012; Kahan et al. 2014). The model space was simplified to the core elements relevant to understand how dopamine modulates intrinsic striatal connectivity. DCM relies on prior assumptions about the distribution of a number of model parameters, but the findings are robust, having being confirmed with an independent model-free analysis.

In this study, we modeled dopaminergic drugs as extrinsic inputs in DCM and demonstrated that these inputs modulate striatal connectivity in a specific topographic fashion. This modulation could be mediated by different elements of mesostriatal circuitry. One possibility is that sulpiride and bromocriptine modulate activity of dopamine cells in the ventral tegmental area (VTA) and substantia nigra pars compacta (SNc). Another possibility is that these drugs modulate D2-receptors in the striatum directly. In theory, it is possible to dissociate between these 2 possibilities by including VTA and SNc as additional nodes in DCM. In practice, it is not possible to get reliable BOLD signals from these regions with the standard whole-brain fMRI settings used in this study. Namely, the anatomical location of these regions makes their BOLD signals exquisitely sensitive to both physiological artifacts and subject motion. The consequences of those artifacts are particularly deleterious during resting-state fMRI. Therefore, we have not included data from these 2 regions in this study and focused on their downstream effects on the striatum. Note that even if dopaminergic drug effects are mediated by modulation of dopamine cells in the midbrain, this does not invalidate the current approach. In this case, we can assume that we have modeled midbrain as a hidden node in DCM and instead of fitting models to data from this region, focused on its downstream effects. This approach has been validated previously in the context of DCM for fMRI [Appendix in Kahan et al. (2014)].

To define regions of interest for DCM, the striatum was parcellated into functionally homogeneous regions using a data-driven method. This connectivity-based parcellation approach overcomes the known difficulty of defining boundaries between functionally distinct regions of the human striatum. For instance, the ventral striatal cluster extended beyond the nucleus accumbens, including the ventromedial caudate nucleus and the rostroventral putamen, in line with neurophysiological studies (Voorn et al. 2004). More generally, our data-driven mediolateral parcellation of the striatum corresponds closely with regions identified on the basis of neurophysiological data, and follows the pattern of excitatory cortical, thalamic, and amygdaloid inputs to the striatum (Alexander et al. 1986; Voorn et al. 2004; Draganski et al. 2008; Haber and Knutson 2010). We limited the main analyses to 3 regions that could be linked to the known mediolateral organization of the striatum and that have been previously shown to be implicated in motivational, cognitive, and premotor circuits (Alexander et al. 1986; Haber et al. 2000; Draganski et al. 2008). A restricted model space generates statistically robust inferences (Penny et al. 2010), but it also limits the inference of this study to ventral and dorsal-anterior portions of the striatum. A post hoc extension of the analyses to the motor striatum, the dorsal-posterior putamen, connections provides strong evidence in favor of a mesostriatal architecture with forward and backward baseline connections between the dorsal-anterior putamen and the dorsal-posterior putamen, with dopamine modulating both connections. These data suggest that dopamine modulates both forward and backward intrastriatal connections along the mediolateral axis of the striatum.

We found evidence that dopamine modulates striatal connectivity not only along the ventral-to-dorsal pathway, but also along the dorsal-to-ventral pathway. At first glance, this finding cannot be reconciled with the model of nigro-striato-nigral connectivity observed in macaques (Haber et al. 2000), which is known to be unidirectional. However, model connections between 2 nodes are not limited to anatomical monosynaptic connections. Accordingly, it is possible that the dorsal striatum might affect the ventral striatum through its connection with the prefrontal cortex. There is neuroanatomical evidence in nonhuman primates that motivational and cognitive areas of the striatum show converging cortical inputs (Haber et al. 2006). Another possibility is that dorsal striatum affects ventral and medial striatum indirectly through its connection via the mediodorsal thalamus, which itself projects to the caudate nucleus (McFarland and Haber 2001, 2002). Indeed, dopaminergic stimulation and blockade of D2-receptors could modulate the thalamus via inhibitory projections from the dorsal striatum to the thalamus, thereby affecting thalamic input of the caudate nucleus.

Conclusion

Building on recent anatomical work (Haber et al. 2000), this study provides empirical evidence for a hierarchical architecture in the flow of information within the human striatum. Communication between the ventral and the dorsal putamen is mediated by the dorsal caudate nucleus. This architecture points to structured interactions between frontostriatal loops that have long been considered to have limited anatomical convergence (Selemon and Goldman-Rakic 1985; Alexander et al. 1986). Furthermore, this study shows how those interactions are modulated by dopaminergic tone. State-related effects, induced by pharmacological interventions, influenced the striatal circuitry along the mediolateral pathway. These effects are consistent with a midbrain-mediated dopaminergic influence on striatal connectivity (Haber et al. 2000). Trait-related effects, indexed by the interaction between impulsivity and pharmacological interventions,

influenced connectivity between the ventral and the dorsal caudate nucleus. This effect is consistent with the notion that impulsivity marks a stronger dopamine-dependent influence of the ventral onto the dorsomedial striatum. One implication of this finding is that, in highly impulsive individuals, early drug intake episodes could quickly lead to goal-directed drug intake (Corbit et al. 2012).

Supplementary Material

Supplementary material can be found at: http://www.cercor.oxfordjournals.org/

Funding

This work was supported by the Innovational Research Incentives Scheme of the Netherlands Organisation for Scientific Research (NWO) with a VIDI grant to R.C., a Human Frontiers Science Program research grant (to Kae Nakamura, R.C. and Nathaniel Daw), a James McDonnell scholar award to R.C. and NWO grant #404-10-062 to I.T. and R.C.

Notes

Conflict of Interest: The authors report no conflict of interest. R.C. is consultant for Abbott Laboratories, but is not an employee or stock shareholder.

Appendix

To ensure that the parcellation scheme is valid at the between-subject level, we performed a stability analysis to identify the largest number of clusters resulting in a clustering solution conserved over subjects. To achieve this, we assessed whether 2 clustering solutions calculated based on 2 independent datasets (e.g., by diving subjects randomly to 2 groups) were matched. Here, we provide a mathematical explanation of our approach.

Two sets of clusters (A and B, each with K clusters) were defined as matched based on the following criteria: First, for every cluster in A and every cluster in B, an overlap index was defined, which corresponds to the number of voxels that overlap between the 2 clusters. Specifically, for every cluster a_i in A and every cluster b_j in B, the overlap index was defined as $N_{i,j}/\min(N_i, N_j)$, where N_i, N_j, and $N_{i,j}$ are the number of voxels in a_i, b_j and their intersection, respectively. Next, for every cluster a_i in A, b_j in B was defined as matched if it had the largest overlap index with a_i. Finally, A and B were considered as matched if each cluster in A was matched with one and only one cluster in B; and vice versa if each cluster in B was matched with one and only one cluster in A. This procedure also gives a one-to-one mapping between "labels" of clusters in A and B, regardless of anatomical location of voxels.

References

Aarts E, van Holstein M, Cools R. 2011. Striatal dopamine and the interface between motivation and cognition. Front Psychol. 2:163.

Alexander GE, DeLong MR, Strick PL. 1986. Parallel organization of functionally segregated circuits linking basal ganglia and cortex. Annu Rev Neurosci. 9:357–381.

Belin D, Everitt BJ. 2008. Cocaine seeking habits depend upon dopamine-dependent serial connectivity linking the ventral with the dorsal striatum. Neuron. 57:432–441.

Belin D, Mar AC, Dalley JW, Robbins TW, Everitt BJ. 2008. High impulsivity predicts the switch to compulsive cocaine-taking. Science. 320:1352–1355.

Biswal B, Yetkin FZ, Haughton VM, Hyde JS. 1995. Functional connectivity in the motor cortex of resting human brain using echo-planar MRI. Magn Reson Med. 34:537–541.

Bond AL, Lader M. 1974. The use of analogue scales in rating subjective feelings. Br J Med Psychol. 47:211–218.

Buckholtz JW, Treadway MT, Cowan RL, Woodward ND, Li R, Ansari MS, Baldwin RM, Schwartzman AN, Shelby ES, Smith CE, et al. 2010. Dopaminergic network differences in human impulsivity. Science. 329:532.

Calzavara R, Mailly P, Haber SN. 2007. Relationship between the corticostriatal terminals from areas 9 and 46, and those from area 8A, dorsal and rostral premotor cortex and area 24c: an anatomical substrate for cognition to action. Eur J Neurosci. 26:2005–2024.

Clatworthy PL, Lewis SJG, Brichard L, Hong YT, Izquierdo D, Clark L, Cools R, Aigbirhio FI, Baron J-C, Fryer TD, et al. 2009. Dopamine release in dissociable striatal subregions predicts the different effects of oral methylphenidate on reversal learning and spatial working memory. J Neurosci. 29:4690–4696.

Cole DM, Beckmann CF, Oei NYL, Both S, van Gerven JMA, Rombouts SARB. 2013. Differential and distributed effects of dopamine neuromodulations on resting-state network connectivity. NeuroImage. 78:59–67.

Cole DM, Oei NYL, Soeter RP, Both S, van Gerven JMA, Rombouts SARB, Beckmann CF. 2013. Dopamine-dependent architecture of cortico-subcortical network connectivity. Cereb Cortex. 23:1509–1516.

Cools R, D'Esposito M. 2011. Inverted-U-shaped dopamine actions on human working memory and cognitive control. Biol Psychiatry. 69:e113–e125.

Cools R, Frank MJ, Gibbs SE, Miyakawa A, Jagust W, D'Esposito M. 2009. Striatal dopamine predicts outcome-specific reversal learning and its sensitivity to dopaminergic drug administration. J Neurosci. 29:1538–1543.

Cools R, Sheridan M, Jacobs E, D'Esposito M. 2007. Impulsive personality predicts dopamine-dependent changes in frontostriatal activity during component processes of working memory. J Neurosci. 27:5506–5514.

Corbit LH, Nie H, Janak PH. 2012. Habitual alcohol seeking: time course and the contribution of subregions of the dorsal striatum. Biol Psychiatry. 72:389–395.

Dalley JW, Everitt BJ, Robbins TW. 2011. Impulsivity, compulsivity, and top-down cognitive control. Neuron. 69:680–694.

Dalley JW, Fryer TD, Brichard L, Robinson ESJ, Theobald DEH, Lääne K, Peña Y, Murphy ER, Shah Y, Probst K, et al. 2007. Nucleus accumbens D2/3 receptors predict trait impulsivity and cocaine reinforcement. Science. 315:1267–1270.

Daunizeau J, Stephan KE, Friston KJ. 2012. Stochastic dynamic causal modelling of fMRI data: should we care about neural noise? NeuroImage. 62:464–481.

Deleu D, Northway MG, Hanssens Y. 2002. Clinical pharmacokinetic and pharmacodynamic properties of drugs used in the treatment of Parkinson's disease. Clin Pharmacokinet. 41: 261–309.

Dodds CM, Clark L, Dove A, Regenthal R, Baumann F, Bullmore E, Robbins TW, Müller U. 2009. The dopamine D2 receptor antagonist sulpiride modulates striatal BOLD signal during the manipulation of information in working memory. Psychopharmacology (Berl). 207:35–45.

Draganski B, Kherif F, Klöppel S, Cook PA, Alexander DC, Parker GJM, Deichmann R, Ashburner J, Frackowiak RSJ.

2008. Evidence for segregated and integrative connectivity patterns in the human basal ganglia. J Neurosci. 28:7143–7152.
Dum RP, Strick PL. 2002. Motor areas in the frontal lobe of the primate. Physiol Behav. 77:677–682.
Everitt BJ, Belin D, Economidou D, Pelloux Y, Dalley JW, Robbins TW. 2008. Review. Neural mechanisms underlying the vulnerability to develop compulsive drug-seeking habits and addiction. Philos Trans R Soc Lond B Biol Sci. 363:3125–3135.
Flitney D, Webster M, Patenaude B, Seidman L, Goldstein J, Tordesillas Gutierrez D, Eickhoff S, Amunts K, Zilles K, Lancaster J, et al. 2007. Anatomical brain atlases and their application in the FSLView visualisation tool. Thirteen Annual Meeting of the Organization for Human Brain Mapping. Chicago, IL, USA.
Fox MD, Raichle ME. 2007. Spontaneous fluctuations in brain activity observed with functional magnetic resonance imaging. Nat Rev Neurosci. 8:700–711.
Friston K, Stephan K, Li B, Daunizeau J. 2010. Generalised filtering. Math Probl Eng. 2010:1–34.
Friston KJ, Li B, Daunizeau J, Stephan KE. 2011. Network discovery with DCM. NeuroImage. 56:1202–1221.
Griswold MA, Jakob PM, Heidemann RM, Nittka M, Jellus V, Wang J, Kiefer B, Haase A. 2002. Generalized autocalibrating partially parallel acquisitions (GRAPPA). Magn Reson Med. 47:1202–1210.
Haber SN, Fudge JL, McFarland NR. 2000. Striatonigrostriatal pathways in primates form an ascending spiral from the shell to the dorsolateral striatum. J Neurosci. 20:2369–2382.
Haber SN, Kim K-S, Mailly P, Calzavara R. 2006. Reward-related cortical inputs define a large striatal region in primates that interface with associative cortical connections, providing a substrate for incentive-based learning. J Neurosci. 26:8368–8376.
Haber SN, Knutson B. 2010. The reward circuit: linking primate anatomy and human imaging. Neuropsychopharmacology. 35:4–26.
He SQ, Dum RP, Strick PL. 1995. Topographic organization of corticospinal projections from the frontal lobe: motor areas on the medial surface of the hemisphere. J Neurosci. 15:3284–3306.
Helmich RC, Derikx LC, Bakker M, Scheeringa R, Bloem BR, Toni I. 2010. Spatial remapping of cortico-striatal connectivity in Parkinson's disease. Cereb Cortex. 20:1175–1186.
Honey GD, Suckling J, Zelaya F, Long C, Routledge C, Jackson S, Ng V, Fletcher PC, Williams SCR, Brown J, et al. 2003. Dopaminergic drug effects on physiological connectivity in a human cortico-striato-thalamic system. Brain J Neurol. 126:1767–1781.
Ikeda H, Saigusa T, Kamei J, Koshikawa N, Cools AR. 2013. Spiraling dopaminergic circuitry from the ventral striatum to dorsal striatum is an effective feed-forward loop. Neuroscience. 241:126–134.
Ikemoto S. 2007. Dopamine reward circuitry: two projection systems from the ventral midbrain to the nucleus accumbens-olfactory tubercle complex. Brain Res Rev. 56:27–78.
Kahan J, Urner M, Moran R, Flandin G, Marreiros A, Mancini L, White M, Thornton J, Yousry T, Zrinzo L, et al. 2014. Resting state functional MRI in Parkinson's disease: the impact of deep brain stimulation on "effective" connectivity. Brain J Neurol. 137:1130–1144.
Kelly RM, Strick PL. 2004. Macro-architecture of basal ganglia loops with the cerebral cortex: use of rabies virus to reveal multisynaptic circuits. Prog Brain Res. 143:449–459.
Lawrence AD, Brooks DJ. 2014. Ventral striatal dopamine synthesis capacity is associated with individual differences in behavioral disinhibition. Front Behav Neurosci. 8:1–6.
Li B, Daunizeau J, Stephan KE, Penny W, Hu D, Friston K. 2011. Generalised filtering and stochastic DCM for fMRI. NeuroImage. 58:442–457.
Lund TE, Nørgaard MD, Rostrup E, Rowe JB, Paulson OB. 2005. Motion or activity: their role in intra- and inter-subject variation in fMRI. NeuroImage. 26:960–964.
McFarland NR, Haber SN. 2001. Organization of thalamostriatal terminals from the ventral motor nuclei in the macaque. J Comp Neurol. 429:321–336.
McFarland NR, Haber SN. 2002. Thalamic relay nuclei of the basal ganglia form both reciprocal and nonreciprocal cortical connections, linking multiple frontal cortical areas. J Neurosci. 22:8117–8132.
Mehta MA, Manes FF, Magnolfi G, Sahakian BJ, Robbins TW. 2004. Impaired set-shifting and dissociable effects on tests of spatial working memory following the dopamine D2 receptor antagonist sulpiride in human volunteers. Psychopharmacology (Berl). 176:331–342.
Neubert F-X, Mars RB, Thomas AG, Sallet J, Rushworth MFS. 2014. Comparison of human ventral frontal cortex areas for cognitive control and language with areas in monkey frontal cortex. Neuron. 81:700–713.
Patton JH, Stanford MS, Barratt ES. 1995. Factor structure of the Barratt impulsiveness scale. J Clin Psychol. 51:768–774.
Penny WD, Stephan KE, Daunizeau J, Rosa MJ, Friston KJ, Schofield TM, Leff AP. 2010. Comparing families of dynamic causal models. PLoS Comput Biol. 6:1–14.
Rigoux L, Stephan KE, Friston KJ, Daunizeau J. 2014. Bayesian model selection for group studies—revisited. NeuroImage. 84:971–985.
Selemon LD, Goldman-Rakic PS. 1985. Longitudinal topography and interdigitation of corticostriatal projections in the rhesus monkey. J Neurosci. 5:776–794.
Shackman AJ, Salomons TV, Slagter HA, Fox AS, Winter JJ, Davidson RJ. 2011. The integration of negative affect, pain and cognitive control in the cingulate cortex. Nat Rev Neurosci. 12:154–167.
Stephan KE, Penny WD, Daunizeau J, Moran RJ, Friston KJ. 2009. Bayesian model selection for group studies. NeuroImage. 46:1004–1017.
van der Schaaf ME, van Schouwenburg MR, Geurts DEM, Schellekens AFA, Buitelaar JK, Verkes RJ, Cools R. 2014. Establishing the dopamine dependency of human striatal signals during reward and punishment reversal learning. Cereb Cortex. 24:633–642.
Voorn P, Vanderschuren LJMJ, Groenewegen HJ, Robbins TW, Pennartz CMA. 2004. Putting a spin on the dorsal-ventral divide of the striatum. Trends Neurosci. 27:468–474.
Wunderlich K, Dayan P, Dolan RJ. 2012. Mapping value based planning and extensively trained choice in the human brain. Nat Neurosci. 15:786–791.

Supporting information

Dopaminergic modulation of the functional ventral-to-dorsal architecture of the human striatum

Payam Piray[1], Hanneke E.M. den Ouden[1], Marieke E. van der Schaaf[1,2], Ivan Toni[1], Roshan Cools[1,2]

[1] Radboud University Nijmegen, Donders Institute for Brain Cognition and Behaviour, Centre for Cognitive Neuroimaging Nijmegen, the Netherlands

[2] Radboud University Medical Centre, Department of Psychiatry, Nijmegen, The Netherlands

Correspondence should be addressed to P.P. (p.piray@donders.ru.nl)

Control analysis with Barratt impulsiveness scale (BIS) in the placebo session as the index of trait impulsivity. We conducted a control analysis using BIS scores in the placebo session (instead of the mean across all four sessions presented in the main text) as the index of trait impulsivity. The results of this control analysis were consistent with those of main analysis.

Similar to the main analysis, a repeated measures ANOVA was employed to assess individual modulatory parameters as a function of connection direction (forward versus backward), striatal pair (ventral striatum and dorsal caudate nucleus or dorsal caudate nucleus and dorsal-anterior putamen) and trait impulsivity (BIS score obtained in the placebo session). Please note that for one of the subjects, BIS was not administered in the placebo session; so data from other subjects were analyzed here. This analysis revealed a significant interaction between trait impulsivity, striatal pair and connection direction ($F(1,22)=4.43$, $p = .047$). Post-hoc correlation analyses revealed that the three-way interaction was due to a highly significant positive correlation between trait impulsivity and the drug effects on the forward connection from the ventral striatum to the dorsal caudate nucleus ($r = 0.51$, $p= 0.01$). Trait impulsivity did not correlate with drug effects on the other connections ($p > 0.05$).

Model-free analysis of trait impulsivity and dopaminergic drug effects on intra-striatal functional connectivity. We conducted a control analysis regarding association of impulsivity with functional connectivity between ventral striatum and dorsal caudate nucleus, which did not depend on the mesostriatal architecture selected from DCM analysis.

Similar to the dynamic causal modeling analysis, the first eigenvariates extracted from the ventral striatum, dorsal caudate nucleus and dorsal-anterior putamen clusters (Figure 1A) were used for analysis. These time-series were employed to compute functional connectivity (correlation) between the striatal regions for each session. First, to quantify the strength of the intra-striatal connections, we computed the average connectivity across the four sessions for each subject and each pair of striatal regions. Next, to quantify the dopaminergic drug effect, we computed the difference in functional connectivity (for each

pair of striatal regions) between the bromocriptine and sulpiride sessions (bromocriptine minus sulpiride). A regression analysis was conducted with the three connections and the three dopaminergic drug effects (on those connections) as predictors (as well as an intercept) and with trait impulsivity as dependent variable (Figure S2A). This analysis investigates the (partial) correlation between each regressor and trait impulsivity while controlling for the variance explained by the other regressors. It revealed that impulsivity was selectively associated with dopaminergic drug effects on the connectivity between ventral striatum and dorsal caudate nucleus ($p=0.027$, Figure S2B, Table S4). The average strength of connections (across drug sessions) did not vary with trait impulsivity, and there was no significant association between impulsivity and drug effects on the two other connections (all $p > .05$, Table S4).

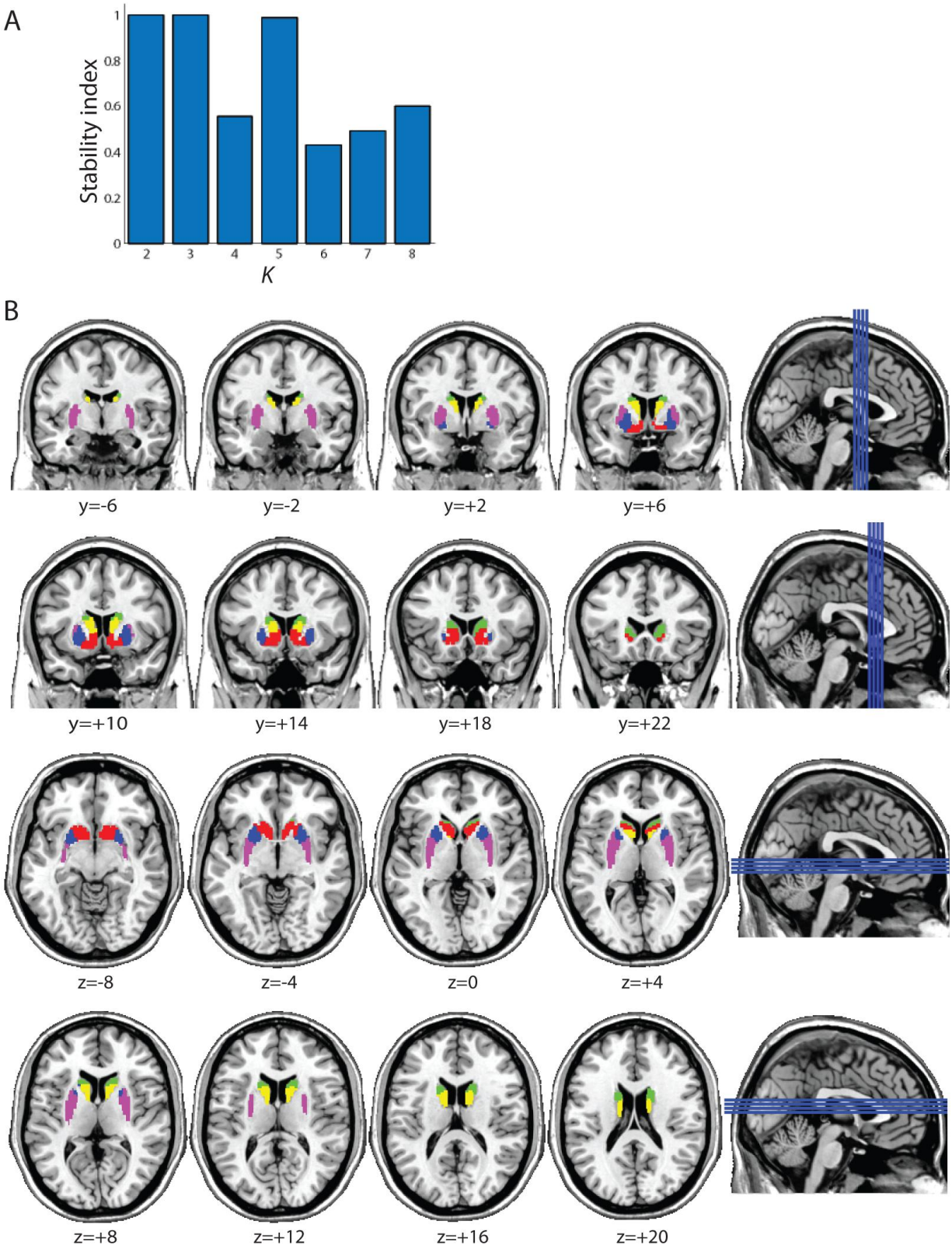
A
Stability index
1
0.8
0.6
0.4
0.2
0
2
3
4
5
6
7
8
K
B
y=-6
y=-2
y=+2
y=+6
y=+10
y=+14
y=+18
y=+22
z=-8
z=-4
z=0
z=+4
z=+8
z=+12
z=+16
z=+20

Figure S1. Parcellation of human striatum based on functional connectivity. A) Stability index as a function of number of clusters, K. The 5-clusters solution is the largest K resulting in stable solution across participants. B) The 5-clusters solution shown in several coronal and axial slices. The clustering solution included a ventral striatal region (including nucleus accumbens, ventral caudate nucleus and ventral parts of the putamen; in red), a medial caudate region (in yellow), a dorsal caudate nucleus region (in green), a dorsal-anterior putamen region (in blue) and a dorsal posterior putamen region (in magenta).

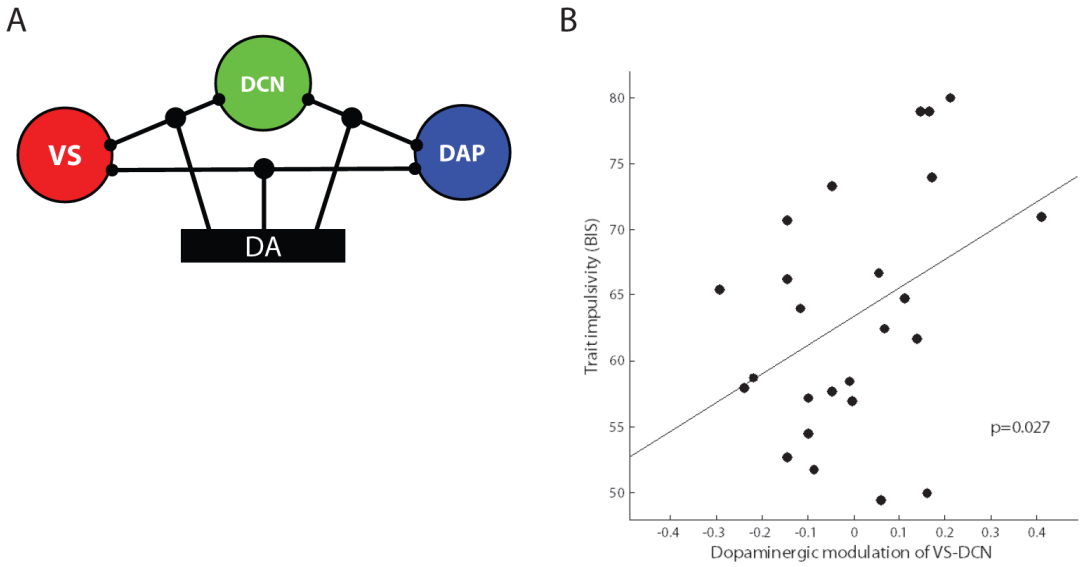

Figure S2. The association between trait impulsivity and dopamine-mediated changes in striatal connectivity obtained from the model-free analysis. A) To quantify the strength of the intra-striatal connections, the functional connectivity between the three striatal regions quantified as the mean correlation across all sessions. The difference in functional connectivity (correlation) between bromocriptine and sulpiride session was used as the dopaminergic drug effects on intra-striatal connectivity. A regression analysis with these six regressors (as well as an intercept) conducted to examine their relationship with trait impulsivity. B) Scatter-plot of the relationship between trait impulsivity (BIS scores) and the dopamine-mediated changes on the coupling between ventral striatum and dorsal caudate nucleus. The values in the x-axis are the differences in the connectivity between bromocriptine and sulpiride sessions (bromocriptine minus sulpiride). The values in the x-axis are adjusted for other regressors. Abbreviations: VS, ventral striatum; DCN, dorsal caudate nucleus; DAP, dorsal-anterior putamen; DA, dopamine; BIS, Barratt impulsiveness scale.

	Placebo	Sulpiride	Bromocriptine	Combined
BIS	63.7 (1.9)	62.6 (1.8)	63.8 (1.9)	64.2 (1.9)

Table S1. Barratt impulsiveness scale (BIS) in each session. Means are shown with standard errors in parentheses.

	VS->DCN	DCN->DAP	DCN->VS	DAP->DCN
A (Hz)	0.1269 (0.018)	0.0820 (0.008)	0.0621 (0.062)	0.1377 (0.138)
B (Hz)	0.0086 (0.0066)	0.0036 (0.0059)	0.0068 (0.0048)	0.0057 (0.0081)

Table S2. Fixed-connection parameters values (A) representing intra-striatal connectivity and dopaminergic-modulatory parameters values (B) of those connections in the winning model, A2B2. Means are shown with standard errors in parentheses. Abbreviations: VS, ventral striatum; DCN, dorsal caudate nucleus; DAP, dorsal-anterior putamen; DA, dopamine; BIS, Barratt impulsiveness scale.

	VS->DCN	DCN->DAP	DCN->VS	DAP->DCN
Effect-size	0.53	0.09	0.37	0.31
p-value	0.007	0.670	0.067	0.138

Table S3. Correlation of dopaminergic-modulatory parameters values in the winning model with Barratt impulsiveness scale (BIS). Effect size is the r-value.

	VS-DCN	DCN-DAP	DCN-DAP
Dopamine-mediated changes in connectivity	21.80 (9.08)*	-14.91 (8.09)	6.86 (13.88)
Baseline intra-striatal connectivity	0.06 (18.09)	37.98 (21.55)	-14.61 (15.67)

Table S4. Model-free analysis of relationship between trait impulsivity and mesostriatal connectivity. Regression coefficients are shown with standard errors in parentheses.